

## Avalanches induced by earthquake in North Tochigi prefecture on 25 February 2013

Hiroki Matsushita<sup>1,\*</sup>, Shinji Ikeda<sup>2</sup>, Yasuhiko Ito<sup>2</sup>, Masaru Matsuzawa<sup>1</sup> and Hiroshi Nakamura<sup>1</sup>

<sup>1</sup>Civil Engineering Research Institute for Cold Region, PWRI, Sapporo, Japan

<sup>2</sup>Snow Avalanche and Land Slide Research Center, PWRI, Myoko, Japan

**ABSTRACT:** We have investigated characteristics of avalanches induced by the North Tochigi Prefecture earthquake with magnitude of 6.3 on February 2012 in Japan and observed snowpack structure at avalanche starting zone. The results indicates that avalanches occurred in entire area along the road with length of about 8 km located on the seismic center and the number of avalanches including small scale collapse of snow on slope was 100 or more. Surface avalanches mostly occurred and had one or two bed surfaces. These bed surfaces corresponded to weak layers which consisted of faceted crystals with low hardness. We also evaluated stability of snowpack on slope under the earthquake and suggested that the avalanches will be induced by decrease in the stability with increase in stress to snowpack due to acceleration caused by the earthquake.

**KEYWORDS:** Earthquake-induced avalanches, Snow pit observation, Stability index

### 1 INTRODUCTION

Earthquake with magnitude of 6.3 occurred in the northern part of Tochigi prefecture, Japan, at 1623 JST on 25 February 2013. The earthquake induced many snow avalanches and landslides around Okukinu-Onsen spa near the seismic center (36.9° N, 139.4° E). In particular, road to the spa was filled due to much snow debris of avalanches, so that 51 persons stayed in the Okukinu-Onsen spa were isolated with no assistance during 24 hours until much snow accumulated on road had been removed from the road.

The earthquake-induced snow avalanches have been reported in Alaska on 27 March 1964 during the Great Alaska Earthquake with magnitude of 9.2; the Western Himalaya, India; the Sakhalin Islands, Russia; Japan and so on. Using the earthquake-induced avalanche events, Podolskiy et al. (2010a) investigated the relationship between the occurrence of the earthquake-induced snow avalanches and the magnitude of earthquake, the distance from the seismic center. Kamiishi et al. (2012) conducted snow pit observations at starting zone of avalanches induced by the North Nagano prefecture earthquake with magnitude of 6.7, occurred on 12 March 2011 in Japan. They also analyzed the stability of snowpack on slope based on the results of the snow pit observations by consider-

ing the horizontal acceleration of seismic ground motion. In addition, there are previous attempts to evaluate the effects of seismic ground motion on the snowpack stability concerning the earthquake-induced avalanche occurrences by theoretical examinations (Ogura et al., 2001; Matsuzawa et al., 2007) and laboratory experiments using shaking-table (Podolskiy et al., 2010b). However, these evaluations for the earthquake-induced avalanche occurrences have not been verified enough because snow profiles obtained by snow pit observation at the starting zone of earthquake-induced avalanches are very few (Higashiura et al., 1979; Ogura et al., 2001; Kamiishi et al., 2012).

In this paper, we investigated characteristics of avalanches induced by the North Tochigi Prefecture earthquake on February 2012 and observed snowpack structure at a starting zone of avalanche. We also considered an effect of seismic ground motion on snowpack stability concerning the occurrence of earthquake-induced avalanche based on the result of snow pit observation.

### 2 CHARACTERISTICS OF AVALANCHES INDUCED BY THIS EARTHQUAKE

#### 2.1 Investigation on avalanche characteristics

Investigation on the characteristics of avalanche occurrence induced by the North Tochigi prefecture earthquake was conducted along the road with length of about 8 km in the Okukinu-Onsen spa (1100 – 1300 m a.s.l.) on 28 February 2013, three days after the earthquake (Figure 1). We attended to the points at bed surface in avalanche starting zone and much debris snow on road. In the investigation, snowpack condition on the level ground was also observed.

---

*Corresponding author address:* Hiroki Matsushita, Civil Engineering Research Institute for Cold Region, PWRI, Sapporo, Japan; tel: +81 11 841 1746; fax: +81 11 841 9747; email: hmatsu@ceri.go.jp

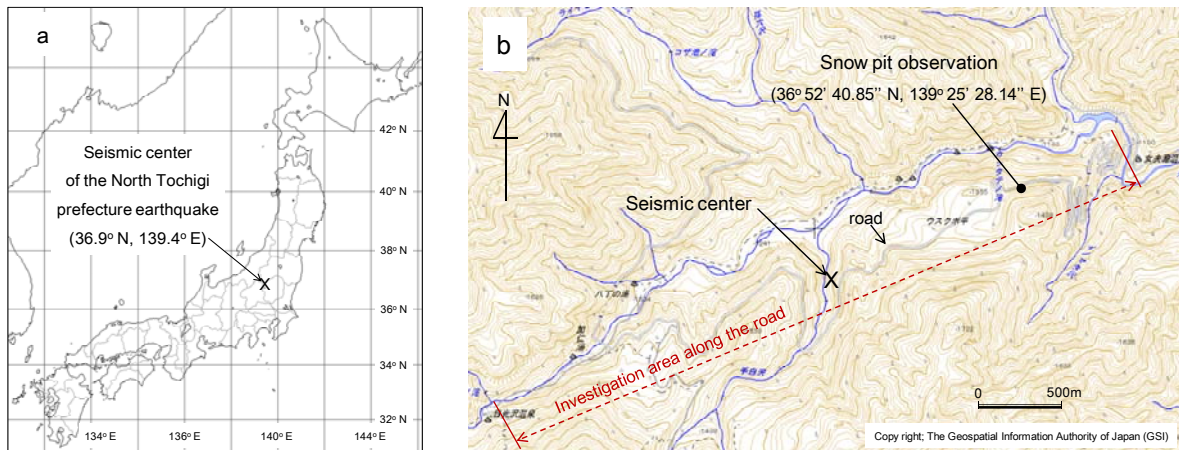


Figure 1. Investigation area and site of snow pit observation.

## 2.2 Characteristics of avalanches

The avalanches induced by this earthquake were observed in the entire area along the road. The number of avalanches including small scale collapse of snow on slope was 100 or more.

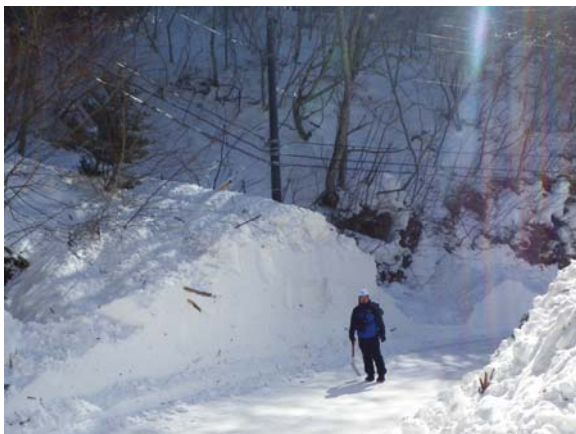


Figure 2. Example of debris snow accumulated on road due to avalanche (1).



Figure 3. Example of debris snow accumulated on road due to avalanche (2).

Debris snow accumulated on the road had the height of 2 m or more (Figure 2) and the length along the road of approximately 60 m (Figure 3) at the areas such as path of valley (Figure 4). Surface avalanches mainly occurred and had one or two bed surfaces (Figures 5 and 6). Crown surfaces of the snow avalanches were stepped and irregular in form. Snowpack failure at its base (like a small full-depth avalanche) and the collapse of block-like snowpack were also confirmed on slope covered with low bamboo bushes and grass (Figures 7 and 8). Cracks were formed at random in snowpack on not only slope (Figure 9), but also level ground (Figure 10).

According to Kamiishi et al. (2012), the characteristics of snow avalanches and collapse of snowpack mentioned above had been also observed as the North Nagano prefecture earthquake occurred on March 2011. Releasing many types of snow avalanches and snow collapses are the characteristics when the earthquake-induced avalanche occurs.

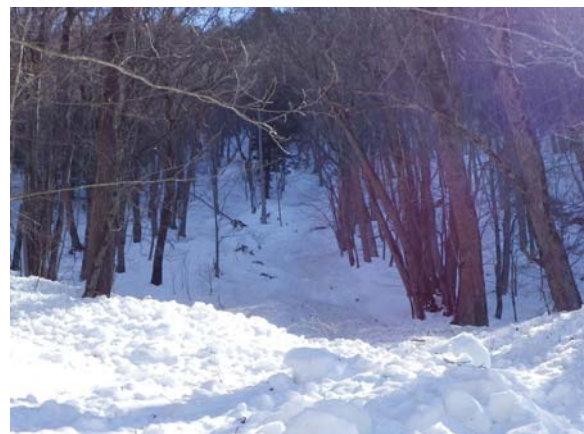


Figure 4. Example of debris snow that passed down on valley.



Figure 5. A case of surface avalanche with single bed surface.



Figure 8. Snowpack failures at its base on the ground surface and collapses of block-like snowpack on slope covered with low bamboo bushes and grass.



Figure 6. A case of surface avalanche with two bed surfaces. Snow pit observation was carried out on this slope.



Figure 9. An example of cracks formed within snowpack at random on slope.



Figure 7. Collapses of block-like snowpack.



Figure 10. An example of cracks formed within snowpack at random on level ground.

### 3 SNOW PROFILE AT STARTING ZONE OF AVALANCHE

#### 3.1 Snow pit observation

We carried out snow pit observation on the slope at starting zone of avalanche ( $36^{\circ} 52' 40.85''$  N,  $139^{\circ} 25' 28.14''$  E) on 28 February 2013 (Figures 1b and 6). Slope incline is  $42^{\circ}$  and aspect of slope is the north. In the snow pit observation, vertical profiles of temperature, density and hardness of snowpack were measured and snow grain's sharp and size were observed. Snow temperature was measured using thermistor thermometer and snow density was obtained by using rectangular sampler with capacity of  $100 \text{ cm}^3$ . Snow hardness was given from measurement of resistance as circular attachment of force gauge with diameter of 15 mm insert into

snowpack (Takeuchi et al., 1998; Höller and Fromm, 2010). Hand test was also carried out to judge the snow hardness for each snow layer. Shape and size of snow grain were observed by using loupe with magnification of 10. In addition, shear frame index (*SFI*) (Perla et al., 1982) was measured for the bed surface of avalanche using the shear frame with area of  $0.025 \text{ m}^2$ . Mean of *SFI*s measured in 5 or 6 times were used.

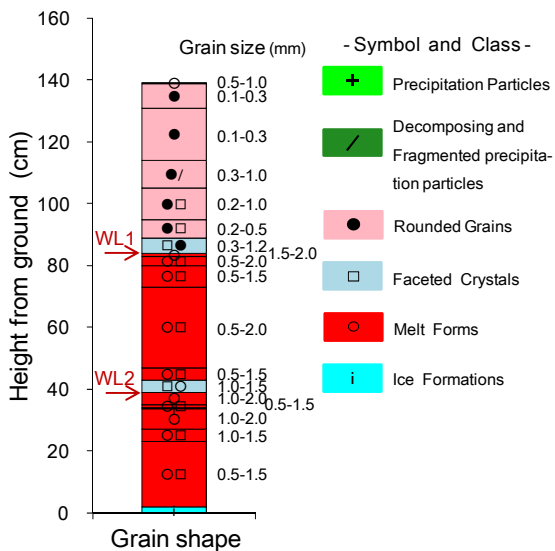


Figure 11. Snow structure at the starting zone of avalanche on 28 February 2013. WL1 and WL2 mean the weak layers 1 and 2, respectively.

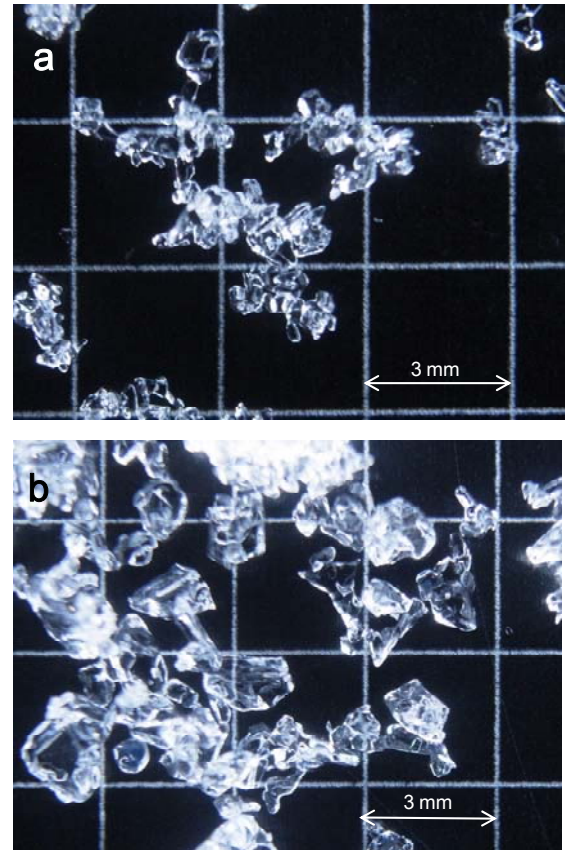


Figure 13. Photographs of snow grains in snow layers at heights of (a) 84 cm and (b) 39 cm from the ground.

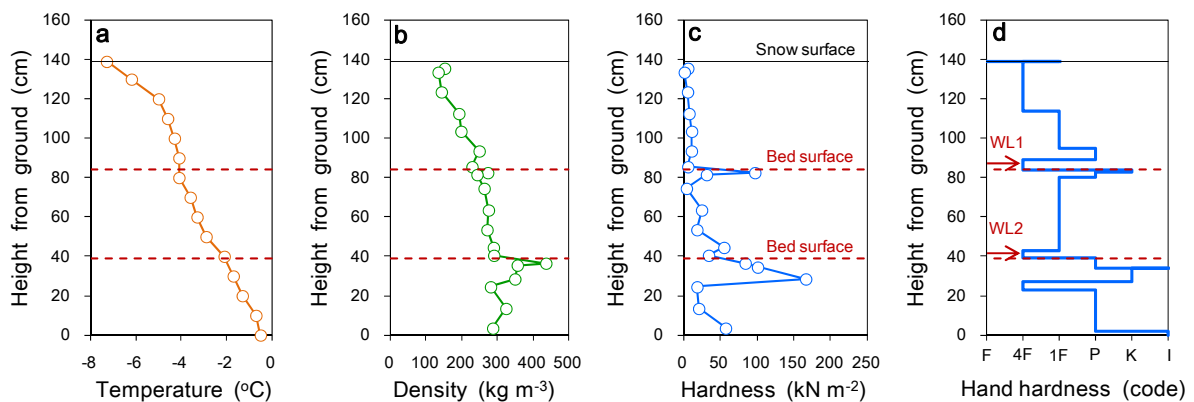


Figure 12. Vertical profiles of (a) temperature, (b) density, (c) hardness and (d) hand hardness of snowpack at the starting zone of avalanche on 28 February 2013. Broken lines indicate the heights of bed surfaces.

### 3.2 Snowpack profile and structure

On slope in where snow pit observation was carried out, there were two bed surfaces and crown surface was formed like a step (Figure 6). Figure 11 shows snowpack structure and Figure 12 indicates vertical profiles of temperature, density and hardness of snow. Snow depth was 139 cm. Snow layers, which correspond to two bed surfaces, were located at heights of 39 cm and 84 cm from the ground and consisted of faceted crystals (Figure 13). Hardness of two snow layers, existed on the bed surfaces, were lower than that of layers above and below (Figures 12c and 12d). In addition, Snow density has changed significantly at two bed surfaces (Figure 12b). Snow layers below the bed surfaces had large hardness and consisted of snow grains of melt forms with large size. Therefore, two snow layers which consisted of faceted crystals would act as weak layers for releasing surface avalanches. We will call the upper and lower weak layers WL1 and WL2. The measured *SFIs* for WL1 and WL2 were 1.51 and 2.89  $\text{kN m}^{-2}$ . The thicknesses *H* of snow layers above the WL1 and WL2 were 0.55 and 1.00 m, respectively.

## 4 SNOWPACK STABILITY AND AVALANCHE INDUCED BY EARTHQUAKE

Using the data obtained from the snow pit observation in the starting zone of avalanche induced by the earthquake, we attempt to evaluate stability of snowpack on slope and will consider the effects of seismic ground motion on the avalanche occurrence.

### 4.1 Method of estimating snowpack stability including the seismic ground motion

Snowpack stability on slope in natural condition can be simply expressed as the ratio of shear stress to shear strength of snow (Figure 14a), so called stability index *SI* given as

$$SI = \frac{\Sigma_s}{\sigma_n \sin \psi} \quad (1)$$

Where  $\Sigma_s$  is the shear strength of weak snow layer ( $\text{N m}^{-2}$ ) and is commonly replaced by the *SFI* ( $\Sigma_s = SFI$ ).  $\sigma_n$  is the normal stress to snow layer per unit area ( $\text{N m}^{-2}$ ) and can be calculated from density  $\rho$  ( $\text{kg m}^{-3}$ ) and thickness *D* (m) of snow layer above the weak layer (i.e.,  $\sigma_n = g\rho D$ ; *g* is the gravitational acceleration ( $\text{m s}^{-2}$ )).  $\psi$  is the slope incline ( $^\circ$ ) and  $\sigma_n \sin \psi$  is the shear stress acting on weak layer.

Seismic ground motion will give rise to stress within snowpack on slope. According to

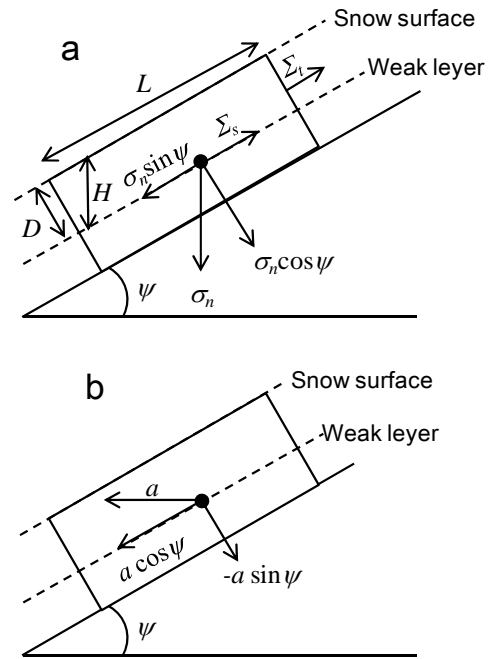


Figure 14. Schematics of (a) stress due to snow weight on weak layer without seismic ground motion, shear strength of weak layer and tensile strength of snowpack above weak layer and (b) shear and normal components of horizontal acceleration against shear plane.

Podolskiy et al. (2010b) and Kamiishi et al. (2012), the stability index *SI* expressed in Equation (1) can be rewritten to the  $SI_E$  given in Equation (2) by considering only horizontal acceleration caused by seismic ground motion (Figure 14b).

$$SI_E = \frac{\Sigma_s}{\sigma_n (\sin \psi + a \cos \psi)} \quad (2)$$

Where *a* is the degree of horizontal acceleration, which is defined as the ratio of the horizontal acceleration caused by seismic ground motion to the gravitational acceleration *g*. In addition to the Equation (2), Matsuzawa et al. (2007) proposed a snow safety factor under earthquake by referring safety factor for slope of soil and the balance of stresses within snowpack on slope under earthquake indicated by Ogura et al. (2001). We rewrote the safety factor proposed by Matsuzawa et al. (2007) to stability index under the earthquake  $SI_E'$  expressed as

$$SI_E' = \frac{CL + \sigma_n L (\cos \psi - a \sin \psi) \tan \phi + \Sigma_s D}{\sigma_n L (\sin \psi + a \cos \psi)} \quad (3)$$

Where *C* is the cohesion factor between snow grains ( $\text{N m}^{-2}$ ),  $\tan \phi$  is the internal friction factor

of snow grain,  $\Sigma_t$  is the tensile strength of snow above the weak layer ( $\text{N m}^{-2}$ ) and  $L$  is the length of snow layer above the weak layer (m) shown in Figure 14a. The tensile strength  $\Sigma_t$  can be obtained from the relation with the snow density provided by Watanabe (1977), for rounded grains, given as

$$\Sigma_t = 3.40 \times 10^{-4} \rho^{3.24}. \quad (4)$$

In Equation (3), the shear strength of snow  $\Sigma_s$  is expressed in form of the Mohr–Coulomb’s expression shown as

$$\Sigma_s = C + \sigma_n \tan \phi. \quad (5)$$

In this paper, the cohesion factor  $C$  is replaced by the  $SFI$  ( $C = SFI$ ). The internal friction factor  $\tan \phi$  should be considered for precipitation particles (PP), decomposing and fragmented precipitation particles (DF) and faceted crystals (FC), but can be neglected for other grain shapes (Jamieson and Johnston, 1998; Yamanoi and

Endo, 2002; Zeidler and Jamieson, 2006; Matsushita et al., 2012). If  $\Sigma_t = 0$  and  $\tan \phi = 0$ , Equation (3) is the same as Equation (2) (i.e.,  $SI_E = SI_E'$ ).

#### 4.2 Effect of seismic ground motion on avalanche occurrence under earthquake

The length of snow layer  $L$  above both the WL1 and WL2 is 9.5 m, the slope incline  $\psi$  is  $42^\circ$ . From the results of the snow pit observation shown in Figure 12, the mean density  $\rho$  and the thickness  $D$  of snow layer accumulated on the WL1 are  $185 \text{ kg m}^{-3}$  and  $0.41 \text{ m}$  ( $= H \cos \psi = 0.55 \text{ m} \cos 42^\circ$ ). Therefore, the normal stress  $\sigma_n$  acting on WL1 is  $0.74 \text{ kN m}^{-2}$ . In the same way, the mean density  $\rho$  and the thickness  $D$  of snow layer accumulated on the WL2 are calculated as  $224 \text{ kg m}^{-3}$  and  $0.74 \text{ m}$  ( $= 1.00 \text{ m} \cos 42^\circ$ ), and the normal stress  $\sigma_n$  acting on WL2 is  $1.62 \text{ kN m}^{-2}$ . The tensile strengths  $\Sigma_t$  of snow layers above WL1 and WL2 are given from Equation (4) using the mean snow density of snow layers above each weak layer. The measured  $SFI$ s for

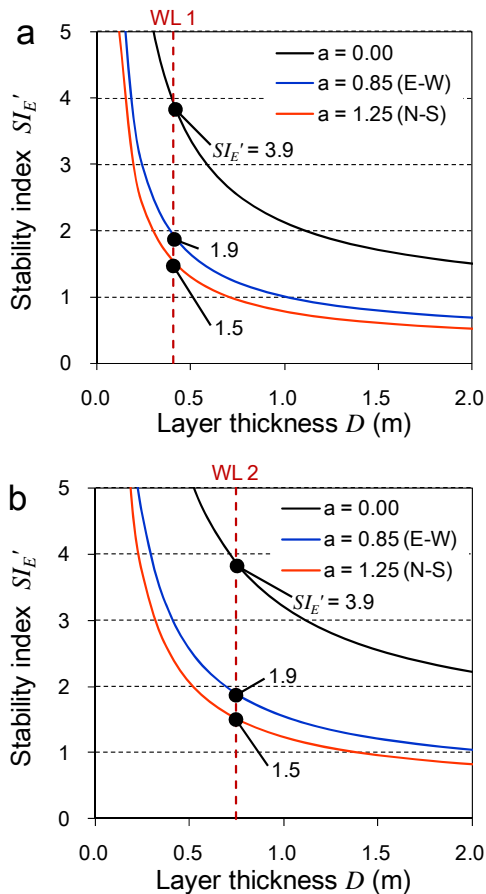


Figure 15. Stability indexes  $SI_E'$  calculated by using Equation (3) for (a) the weak layer 1; WL1 and (b) the weak layer 2; WL2. The  $a$  is the degree of horizontal acceleration.

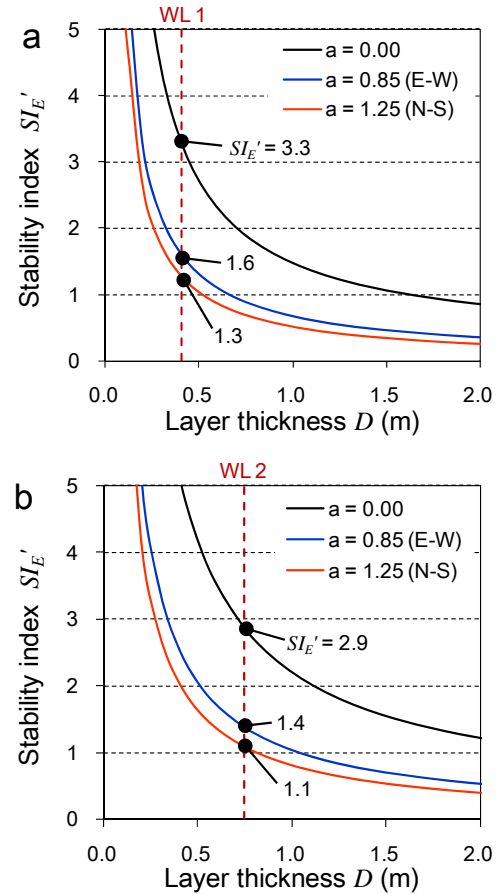


Figure 16. The same as Figure 15 except for the condition after crack formation within snow-pack ( $\Sigma_t = 0$ ).

WL1 and WL2 are used as the cohesion factors  $C$ . The internal friction factor  $\tan\phi$  is chosen to be 0.21 for faceted crystals found by Zeidler and Jamieson (2006).

Acceleration of ground motion caused by the earthquake have been recorded at Kuriyamashi (36.882° N, 139.453° E) of the KIK-net of the National Research Institute for Earth Science and Disaster Prevention (NIED), located at distance of about 4 km from the seismic center. The maximum values of horizontal accelerations recorded at this site are 12.24 m s<sup>-2</sup> ( $a = 1.25$ ) in the direction of N-S and 8.35 m s<sup>-2</sup> ( $a = 0.85$ ) in the direction of W-E.

Substituting these values mentioned above for Equation (3) gives the stability index of snowpack on slope under the earthquake  $SI_E'$  (Figure 15). As seen in Figure 15, in the condition of no seismic ground motion ( $a = 0$ ), the stability indexes  $SI_E'$  for WL1 and WL2 are the same as 3.9. However, in the maximum value of the degree of horizontal acceleration observed ( $a = 1.25$ ), both the stability indexes  $SI_E'$  for WL1 and WL2 decrease to 1.5. Therefore, the horizontal acceleration caused by the earthquake add the shear stress to snowpack on slope and the avalanches will be induced due to the decrease in the stability.

The stability index  $SI_E'$  after crack formation within snowpack is also calculated (i.e.,  $\Sigma_t = 0$  in Equation (3)) and is shown in Figure 16. In the case of the degree of horizontal acceleration  $a = 1.25$ , the stability indexes  $SI_E'$  for WL1 and WL2 are 1.3 and 1.1, respectively. If the crack formed within snowpack (it may occur due to the vertical acceleration caused by the earthquake), the snowpack on slope would be more unstable under the earthquake.

Kamiishi et al. (2012) has estimated that the stability index  $SI_E$  for the weak layer which consisted of wet granular grains of melt forms under the North Nagano prefecture earthquake on 2011 was 1.5 or less, using Equation (2) (i.e., Equation (3) with  $\tan\phi=0$  and  $\Sigma_t = 0$ ).

Consequently, the stability index can be used for evaluating the effect of seismic ground motion on avalanche occurrence.

## 5 CONCLUSION

We have investigated the characteristics of avalanches induced by the North Tochigi Prefecture earthquake on February 2012 and observed snowpack structure at avalanche starting zone. The results indicated that avalanches occurred in entire area along the road with length of about 8 km located on the seismic center and the number of avalanches including small scale collapse of snow on slope was 100 or more. Surface avalanches mostly occurred and had

one or two bed surfaces. These bed surfaces corresponded to the weak layer consisted of faceted crystals with low hardness. We also evaluated the stability of snowpack on slope and suggested that the horizontal acceleration caused by the earthquake add the shear stress to snowpack on slope and the avalanches will be induced due to the decrease in the stability of snowpack on slope.

However, the vertical motion caused by the earthquake will also affect the failure of snowpack on slope (Podolskiy et al., 2010b; Matsushita et al., 2013). To better understanding of mechanism of snowpack failure under the earthquake, we will conduct an experiment using snow-block on vibration table, which can be control the acceleration and period of the vibration, and will obtain the data on the response characteristics of snowpack to the ground motion and on the snowpack failure (e.g., Matsushita et al., 2013).

## ACKNOWLEDGMENTS

We thank the Nikko Sabo Office of the Ministry of Land, Infrastructure, Transport and Tourism (MLIT) and the Nikko City for cooperation to our field investigation. We also acknowledge Emi Nakamura, the Snow Avalanche and Land Slide Research Center, for support during the field investigation, and Dr. Isao Kamiishi, the National Research Institute for Earth Science and Disaster Prevention (NIED), for providing the information on the earthquake-induced snow avalanches.

## REFERENCES

- Higashiura, M., Nakamura, T., Nakamura, H. and Abe, O., 1979. An avalanche caused by an earthquake. Rep. Nat. Res. Cent. Disaster Prev., 21: 103-112. [In Japanese with English abstract]
- Höller, P. and Fromm, R., 2010. Quantification of the hand hardness test. Ann. Glaciol., 51: 39-44.
- Jamieson, J.B. and Johnston, C.D., 1998. Refinements to the stability index for skier-triggered dry-slab avalanches. Ann. Glaciol., 26: 296-302.
- Kamiishi, I., Motoyoshi, H., Ishizaka, M. and Sato, T., 2012. Avalanches induced by North Nagano Prefecture Earthquake on 12 March 2011. J. Jpn. Soc. Snow Ice (Seppy), 74: 159-169. [In Japanese with English abstract]
- Matsushita, H., Matsuzawa, M. and Abe, O., 2012. The influences of temperature and normal load on the shear strength of snow consisting of precipitation particles. Ann. Glaciol., 61: 31-38.
- Matsushita, H., Harada, Y., Kasamura, S., Matsuzawa, M. and Nakamura, H., 2013. Experiment on response characteristics of snowpack on slope to earthquake motion. Proc. JSSI & JSSE Joint Conference 2013 in Kitami: (submitted). [In Japanese]

- Matsuzawa, M., Kajiya, Y. and Ito, Y., 2007. Assessment of snow safety factor under earthquake. *Snow Ice Hokkaido (Hokkaido no Seppyo)*, 26: 95-98. [In Japanese]
- Ogura, Y., Izumi, K., Miyazaki, N. and Kobayashi, S., 2001. An avalanche caused by an earthquake at Nakazato village, Niigata Prefecture, on January 4th 2001. *Ann. Rep. Saigai-ken, Niigata Univ.*, 23: 9-15. [In Japanese with English abstract]
- Perla, R., Beck, T.M.H. and Cheng, T.T., 1982: The shear strength index of alpine snow. *Cold Reg. Sci. Technol.*, 6: 11-20.
- Podolskiy, E.A., Nishimura, K., Abe, O. and Chernous, P.A., 2010a. Earthquake-induced snow avalanches: I. Historical case studies. *J. Glaciol.*, 56: 431-446.
- Podolskiy, E.A., Nishimura, K., Abe, O. and Chernous, P.A., 2010b: Earthquake-induced snow avalanches: II. Experimental study. *J. Glaciol.*, 56: 447-458.
- Takeuchi, Y., Nohguchi, Y., Kawashima, K. and Izumi, K., 1998. Measurement of snow-hardness distribution. *Ann. Glaciol.*, 26: 27-30.
- Watanabe, Z., 1977. The influence of snow quality on the breaking strength. *Sci. Rep. Fukushima Univ.*, 27: 27-35.
- Yamanoi, K. and Endo, Y., 2002. Dependence of shear strength of snow cover on density and water content. *J. Jpn. Soc. Snow Ice (Seppyo)*, 64: 443-451. [In Japanese with English abstract]
- Zeidler, A. and Jamieson, B., 2006. Refinements of empirical models to forecast the shear strength of persistent weak snow layers: Part A: Layers of faceted crystals. *Cold Reg. Sci. Technol.*, 44: 194-205.